NONLINEAR MAGNETICS

by

Nasir Uddin Ahmed

submitted to the Dept. of Electrical Engg., University of Ottawa,
in partial fulfillment of the requirements for the degree of
Master of Science

Department of Electrical Engineering
Faculty of Pure and Applied Science
The University of Ottawa
Ottawa, Canada
1963.

ACKNOWLEDGEMENT

The author wishes to thank professor G.S. Glinski, who suggested and supervised the project.

The author also thanks Miss Olga Boshko for her assistance in computations.

Thanks are also due to the Atomic Energy Commission of Pakistan and Colombo Plan of Canada who sponsored the project.

CONTENTS

ABSTRACT

The purpose of this work is to provide a probabilistic interpretation of magnetization processes of polycrystalline ferromagnetic specimens.

In chapter I, some basic properties of normal and lognormal probability functions are briefly described as far as they are needed in this work.

In chapter II, a probabilistic method is developed for the analysis of magnetization curves and hysteresis loops of polycrystalline materials.

The principal results of this investigation are (i) magnetization by reversible and irreversible wall motion satisfy normal distributions and magnetization by domain rotation satisfies lognormal distributions, (ii) the differential permeability curves corresponding to magnetization curves or hysteresis loops can be expressed as sums of appropriately weighted normal and lognormal probability functions.

The computational procedures are briefly described in the appendices.

CHAPTER I

SOME PROBABILITY FUNCTIONS

1.1 Introduction

In this chapter, is presented a brief discussion of some of the basic properties of two probability functions that were found useful in this work.

1.2 Normal Distribution

A random variable ξ is said to have Gaussian distribution if the probability that ξ assumes a value $x \leq X$ is given by the following expression

$$P_{\xi}\,[x \leq X] = \int_{-\infty}^{X} \frac{1}{\sigma\sqrt{2\pi}} \exp\left\{-\frac{1}{2}\left[\frac{(x-m)^2}{\sigma^2}\right]\right\} dx \qquad (1.1)$$

The corresponding probability density function is,

$$p_{\xi}(x) = \frac{1}{\sigma\sqrt{2\pi}} \exp\left\{-\frac{1}{2}\left[\frac{(x-m)^2}{\sigma^2}\right]\right\} \qquad (1.2)$$

where m is the mean and σ^2 is the variance of the ~~process~~ random variable ξ. The variance gives the measure of dispersion of the ~~process~~ random variable ξ from its mean.

Some important properties of the probability function $p_{\xi}(x)$ are:-

$$\text{(i)} \int_{-\infty}^{+\infty} p_{\xi}(x)\, dx = 1 \qquad (1.3)$$

(ii) $p_\xi(x)$ is a symetric function of x about x = m.

(iii) as σ increases $p_\xi(x)$ becomes flatter and flatter (Fig. 1.1) i.e. the deviation of ξ from its mean m increases indefinitely as $\sigma \to \infty$.

(iv) as $\sigma \to o$, $p_\xi(x) \longrightarrow \delta(x-m)$ (1.4)

(v) as $\sigma \to \infty$, $p_\xi(x) \longrightarrow o$ for all $|x| < \infty$

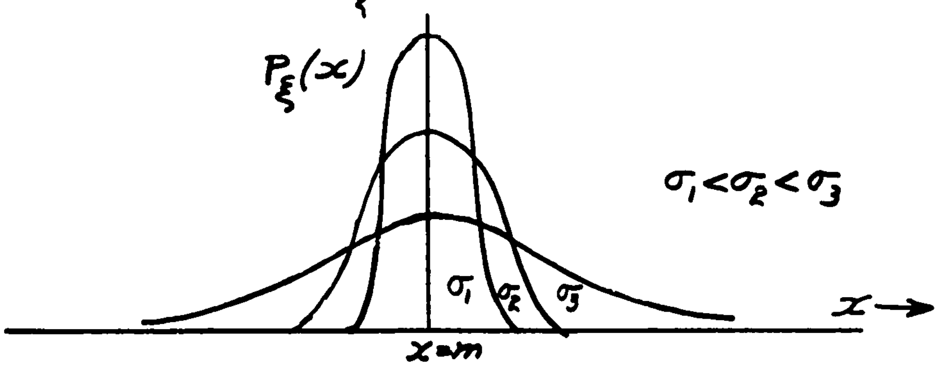

Fig. 1.1 Normal Density Function for Different Values of σ

That m and σ^2, in equation 1.2, are the mean and variance respectively, can be verified by the use of characteristic functions. Characteristic function is defined as,[2]

$$\varphi(t) = \langle e^{itx} \rangle_{av} = \int_{-\infty}^{+\infty} p_\xi(x)\, e^{itx}\, dx \tag{1.5}$$

In fact, $\varphi(t)$ and $p_\xi(x)$ are Fourier transforms[2] of each other i.e.

$$\varphi(t) = \int_{-\infty}^{+\infty} p_\xi(x)\, e^{itx}\, dx \tag{1.6}$$

$$p_\xi(x) = \int_{-\infty}^{+\infty} \varphi(t)\, e^{-itx}\, dt \tag{1.7}$$

Use of characteristic functions as defined above simplifies the study of many properties of probability functions.

If the integral in 1.6 is uniformly convergent and if the moments of order n exist for the process ξ then we can interchange the order of differentiation and integration and obtain the n-th derivative of $\varphi(t)$ as

$$\varphi^{(n)}(t) = \int_{-\infty}^{+\infty} p_{\xi}(x)\,(ix)^n\, e^{itx}\, dx \qquad (1.8)$$

The nth order moment of the process ξ is then given by,

$$\langle x^n \rangle = \left. \frac{\varphi^{(n)}(t)}{i^n} \right|_{t=o} \qquad (1.9)$$

For processes, satisfying normal probability law, moments of all (finite) order exist. For normal probability function, $\varphi(t)$ is given as $\varphi(t) = e^{itm}\, e^{-\frac{t^2 \sigma^2}{2}}$ (1.10)

Using 1.9 and 1.10 for n = 1 and 2, it can be shown that

$$\langle x \rangle = \left. \frac{\varphi^{(1)}(t)}{i} \right|_{t=o} = m \qquad (1.11)$$

and

$$\langle x^2 \rangle = \left. \frac{\varphi^{(2)}(t)}{i^2} \right|_{t=o} = m^2 + \sigma^2 \qquad (1.12)$$

The variance of the normal process is given by

$$\langle (x - \langle x \rangle)^2 \rangle = \sigma^2 \qquad (1.13)$$

The properties (i) through (iii) are quite clear, property (iv) and (v) can be verified as follows:-

$$\lim_{\sigma \to o} p_{\xi}(x) = \lim_{\sigma \to o} \int_{-\infty}^{+\infty} \varphi(t)\; e^{-itx}\, dt$$

$$= \int_{-\infty}^{+\infty} \lim_{\sigma \to o} \varphi(t)\; e^{-itx}\, dt$$

$$= \int_{-\infty}^{+\infty} e^{it(x-m)}\, dt = \delta(x-m) \qquad (1.14)$$

This proves the property (iv). Similarly it can be proved that for any finite x i.e. $|x| < \infty$,

$$\lim_{\sigma \to \infty} p_{\xi}(x) = o. \qquad (1.15)$$

The property (iv) states that the random variable ξ assumes the value m almost surely and (v) states that the random variable ξ assumes no finite value, which will be interpreted as almost certain nonappearance of the process ξ .
These properties will be found useful in the interpretation of square hysteresis loops.

1.3 Lognormal Distribution.

This is a special case of transformed normal [2] distribution. If x is a random variable and if a certain function of x satisfies normal distribution, the corresponding distribution may be called a transformed normal distribution.

Let $g(x)$ be the function of x, that satisfies normal distribution. Then one can write

$$p(x)\, d\, g(x) = \frac{1}{\sigma\sqrt{2\pi}} \exp\left\{- \frac{1}{2}\left[\left(\frac{g(x) - m}{\sigma}\right)^2\right]\right\} d\, g(x). \qquad (1.16)$$

The corresponding distribution function denoted by F(x) is given by

$$F(x) = \int_{-\infty}^{x} p(g(z))dg(z) = \int_{-\infty}^{x} \frac{1}{\sigma\sqrt{2\pi}} \exp\left\{-\frac{1}{2}\left[\left(\frac{g(z)-m}{\sigma}\right)^2\right]\right\}dg(z) \qquad (1.17)$$

If g(x) is assumed continuous over $(-\infty, +\infty)$ then F(x) can be written as

$$F(x) = \int_{-\infty}^{x} \frac{1}{\sigma\sqrt{2\pi}} \exp\left\{-\frac{1}{2}\left[\left(\frac{g(z)-m}{\sigma}\right)^2\right]\right\}g'(z)dz. \qquad (1.18)$$

A special case of considerable importance in the study of hereditary phenomenon, magnetic hysteresis and saturation etc. is where

$$g(x) = \begin{cases} \log(x-a) & \text{for } x > a \\ 0, & x \leq a \end{cases} \qquad (1.19)$$

In this case equation 1.18 becomes

$$F(x) = \int_{a}^{x} \frac{1}{\sigma\sqrt{2\pi}(z-a)} \exp\left\{-\frac{1}{2}\left[\left(\frac{\log(z-a)-m}{\sigma}\right)^2\right]\right\}dz \qquad (1.20)$$

Therefore, the corresponding probability function is

$$p(x) = \frac{1}{\sigma\sqrt{2\pi}(x-a)} \exp-\frac{1}{2}\left[\left(\frac{\log(x-a)-m}{\sigma}\right)^2\right] \qquad (1.21)$$

for all $x > a$; and

$$p(x) = 0 \text{ for } x \leq a.$$

This is known as lognormal probability function.

One important point to be noted is that the mean, m is measured always from x = a. Thus, to obtain the absolute mean measured from the origin, one must add the parameter a to m.

That is, $m_a = m + a$. This is illustrated in the figures 1.2 and 1.3

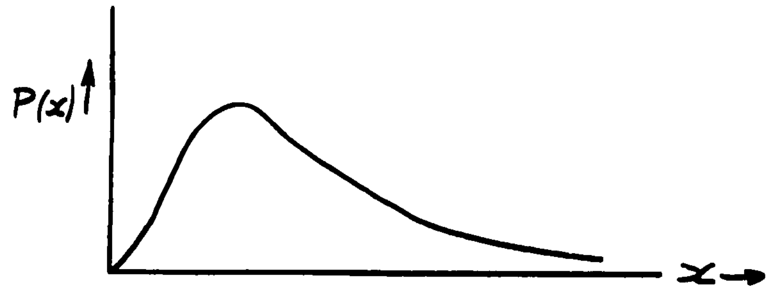

Fig. 1.2: $a = o$ and $m_a = m$.

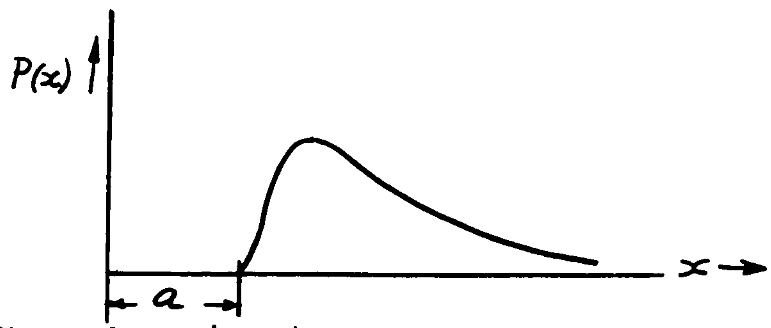

Fig. 1.3: $a \neq o$, and $m_a = m + a$.

This probability function has a similar set of properties as described before for the normal distribution.

(i) $\int_a^\infty p(x)\ dx = 1$

(ii) The lognormal density function is an unsymmetrical function unlike the normal density function.

(iii) As σ increases, p(x) becomes flatter and flatter; i.e. the deviation of the random variable x from its mean increases indefinitely as $\sigma \rightarrow \infty$.

(iv) As $\sigma \rightarrow 0$

$$p(x) \rightarrow \delta\,[\,x - (a+e^m)\,]$$

(v) As $\sigma \rightarrow \infty$, $p(x) \rightarrow 0$ for all $|x| < \infty$

These properties can be proved as before.

1.4 Series Representation of Arbitrary Probability Functions.

In statistical studies it is sometimes necessary to approximate an experimental distribution curve by means of known distribution functions. This can often be done conveniently by use of the property of bi-orthogonality that exists between Hermite polynomials and the normal probability function and its derivatives. Let us consider normal distribution with unit σ and zero mean:

$$\psi(x) = \frac{1}{\sqrt{2\pi}} e^{-\frac{x^2}{2}} \tag{1.22}$$

By taking its derivatives with respect to x it can be shown that

$$\psi^{(n)}(x) = \frac{(-1)^n}{\sqrt{2\pi}} e^{\frac{-x^2}{2}} \cdot H_n(x) \tag{1.23}$$

where $H_n(x)$, is the nth degree Hermite polynomial [1] and is given by

$$H_n(x) = (-1)^n e^{\frac{x^2}{2}} \frac{d^n}{dx^n}(e^{-\frac{x^2}{2}}) \tag{1.24}$$

It can be proved that

$$\int_{-\infty}^{+\infty} H_n(x)\psi^{(m)}(x)\, dx = 0 \quad \text{for } m \neq n$$
$$= (-1)^n \Gamma(n+1) \text{ for } m = n \tag{1.25}$$

Thus, given any experimental probability function, it is often possible to approximate it by a uniformly convergent series, known as Gram charlier series

i.e.

$$P_o(x) = \lim_{n \to \infty} \sum_{k=o}^{n} C_k \psi^{(k)}(x). \tag{1.26}$$

where $P_o(x)$ is the experimental probability function.
The coefficients $\{C_n\}$ are obtained from the following integral

$$C_n = \frac{(-1)^n}{\Gamma(n+1)} \int_{-\infty}^{+\infty} H_n(x)\; P_o(x)\; dx. \tag{1.27}$$

CHAPTER II

PROBABILISTIC INTERPRETATION OF MAGNETIZATION PROCESSES IN POLYCRYSTALLINE SPECIMENS OF FERROMAGNETIC MATERIALS.

2.1 Introduction.

We are interested in presenting an analytical expression of magnetization processes of polycrystalline materials. According to the domain theory, the magnetization curves of magnetic specimens are obtained by minimizing the sum of magnetocrystalline energy [4], magnetostriction energy [4] and the energy due to applied magnetic field. For magnetocrystalline and magnetostriction energies, one uses formulae due to Akulov [3]. By use of this method, magnetization curves of single crystal specimens of iron, nickel, etc. have been obtained [3]. These results agree well with the experimental ones. In the case of polycrystalline specimens this method proves to be unsatisfactory.

The method presented in this thesis consists of expressing the differential permeability curves [6] corresponding to magnetization curves and hysteresis loops as a weighted sum of probability functions assigned to each of the magnetization processes.

2.2 Magnetization Processes.

Three distinct processes [5] are known to contribute to the total magnetization of a ferromagnetic specimen,

(i) Reversible wall motion

(ii) Irreversible wall motion.

(iii) Domain rotation.

(i) Magnetization by reversible wall motion usually takes place at very small fields.

For illustration, a single crystal specimen is considered with domain arrangements as shown in Fig. 2.1. The figure shows 90° domain walls as thin lines separating the rectangles, as the domains.

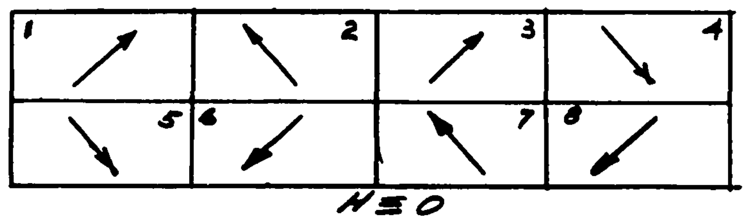

Fig. 2.1. Arrangement of 90° walls in single crystals.

With the application of a small field $H = H_s$ in the direction as indicated(Fig. 2. 2), the domain wall moves and the domains marked (1) - (4) expand at the expense of those marked (5) - (8), resulting in a change of state as shown in Fig. 2.2.

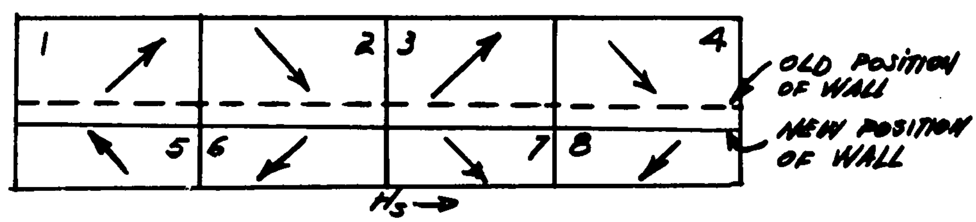

Fig. 2.2: Wall position ----old —— new.

(ii) Magnetization by irreversible wall motion takes place at some intermediate fields. Sufficiently strong field may cause the wall to move to the boundaries of the crystal as shown in Fig. 2.3.

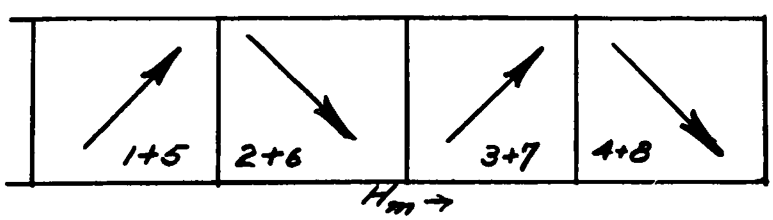

Fig. 2.3: Wall position in intermediate field.

(iii) As the magnetic field is further increased magnetization can take place only by rotation of domains towards the direction of the applied field H. This requires relatively larger field, because the domains are turned through various crystallographic axes, which are essentially the hard directions of magnetization. This is illustrated in Figure 2.4.

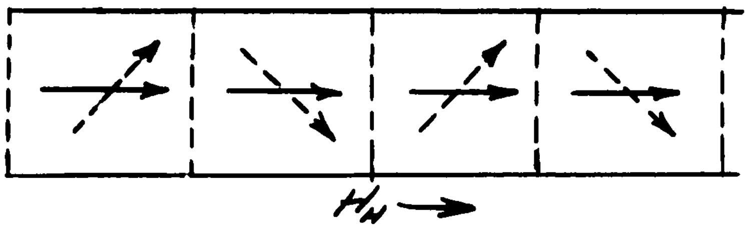

Fig. 2.4: Domain rotation in high field.

The dotted lines indicate the previous state as shown in Figure 2.3. From this brief consideration it is now possible to explain the technical magnetization curve (Fig. 2.5) as follows. With the application of a small magnetic field, magnetization takes place by reversible boundary displacement (wall motion) and with the withdrawal of the field, magnetization reduces to zero. This is a reversible process. If, instead, the field is increased further, magnetization may take place by irreversible boundary displacement and simply reducing the magnetic field H to zero will no longer reduce the magnetization to zero. This is known as irreversible process. Here, energy is spent in raising the temperature of the lattice.

If the magnetic field is relatively high, magnetization takes place by domain rotation until all the domains are perfectly aligned in the direction of the applied field. These are illustrated in Figure 2.5.

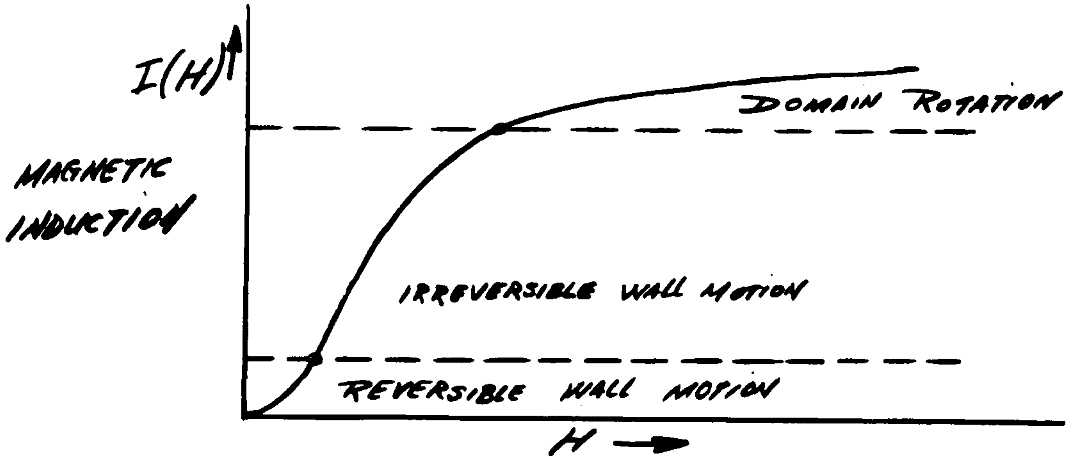

Fig. 2.5: A typical magnetization curve.

2.3 Origin of Hysteresis.

Hysteresis can be better explained from the consideration of equilibrium wall position in a specimen. Owing to the random distribution of impurity centres and stresses, all positions in the specimen are not stable for occupation by domain walls. The Domain wall can occupy only those positions where the total energy is a minimum. The spatial derivative of energy versus wall position [4] may take the form as shown in Figure 2.6.

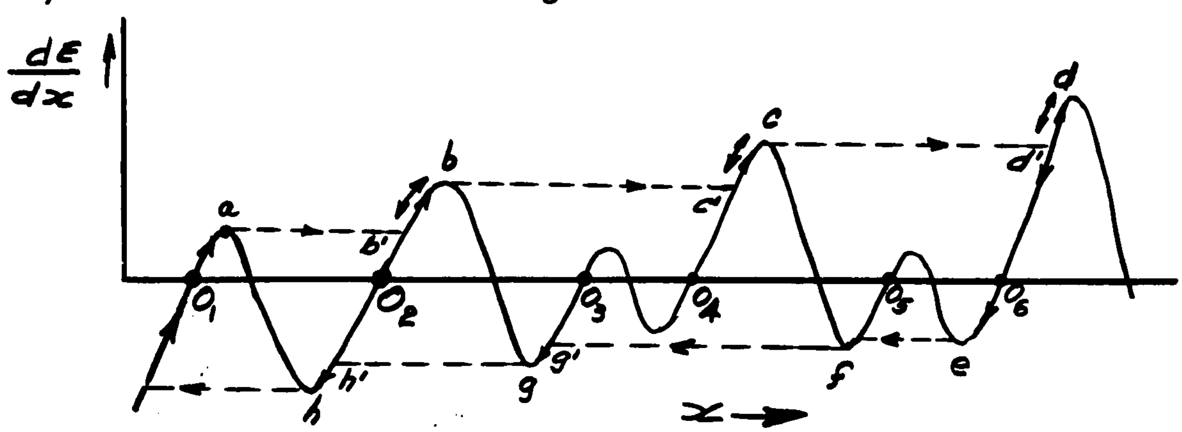

Fig. 2.6: Spatial rate of charge of energy versus wall position.

The positions marked 0_i are the stable equilibrium positions for occupation by domain walls where E is minimum and the slope of $\frac{dE}{dx}$ is positive. The line, $\frac{dE}{dx} = 0$, moves by an amount proportional to the applied field H. With the application of an external field H, a wall occupying the position 0_1 moves along 0_1 a and as the field continues to increase, the wall makes unstable jumps known as Barkhausen jumps [6] at points marked a, b, c, etc and reaches position marked d'. If the field is reduced at this stage, the wall returns along $d'0_6$ and finally reaches the position 0_1 along the dotted lines e f g h. The paths 0_1a, 0_2b, etc are reversible. The area enclosed by the dotted envelope represents the loss of energy in the lattice in returning the wall to its initial position 0_1. The relations, $x \propto I$, and $\frac{dE}{dx} \propto H$, indicate that the dotted curve, when rotated by 90^o, represents the familiar hysteresis loop. With this brief discussion, now we consider the mathematical model developed for magnetization processes of Polycrystalline specimens.

2.4. Assumptions For Mathematical Model.

The mathematical model developed is based on the following assumptions:-

(i) The domains in any given specimen are randomly oriented and the distribution of impurity centres and stresses in the material is also random.

(ii) each of the three distinct processes, reversible wall motion, irreversible wall motion and domain rotation contributing to the total magnetization of a specimen, satisfy certain statistical distributions.

(iii) the correlation between the three processes is negligible.

(iv) $\frac{I(H)}{I_s}$ versus H curve can be regarded as the cumulative distribution of domain orientation, i.e the probability, that a fraction $F(H) = \frac{I(H)}{I_s}$, of the total number of domains will contribute to the overall magnetization I(H), is $F(H) = \int_0^H p(H)dH$.

Hence $$p(H) = \frac{1}{I_s} \frac{dI(H)}{dH}. \tag{2.1}$$

Mathematical models for magnetization curves and hysteresis loops developed on the basis of the above assumptions are presented in the following sections.

2.5 Magnetization Curves.

The differential permeability curve as obtained from the first derivative of a magnetization curve with respect to the field strength H, is expressed as a sum of three components, each component representing one of the three basic processes of magnetization.

Thus, $$p_o(H) = \sum_{i=1}^{3} A_i P_i (H) \tag{2.2}$$

where, $p_o(H)$ is the differential permeability of the specimen and $p_i(H)$, i = 1, 2, 3, are the probability functions associated with the three magnetization processes. $\{A_i\}$ are the appropriate scaling factors. The probability functions $\{P_i(H)\}_{i=1}^{3}$ are as follows:-

$$P_1(H) = \frac{1}{\sigma_1\sqrt{2\pi}} \exp - \frac{1}{2} [(\frac{H - m_1}{\sigma_1})^2] \tag{2.3}$$

$$P_2(H) = \frac{1}{\sigma_2 \sqrt{2\pi}} \exp - \frac{1}{2} [(\frac{H-m_2}{\sigma_2})^2] \tag{2.4}$$

and

$$P_3(H) = \frac{1}{\sqrt{2\pi}\,\sigma_3 (H - H_m)} \exp - \frac{1}{2} \left[\left(\frac{\log(H-H_m) - m_3}{\sigma_3} \right)^2 \right] \qquad (2.5)$$

In these, the first two represent magnetization through the processes of reversible and irreversible wall motion respectively, and the last component represents magnetization through the process of domain rotation. The symbols, σ_i^2, m_i, etc represent variance and mean of the i-th process and H_m represents the minimum field strength necessary for domain rotation to start. The expression, equation 2.2, has been used to represent the differential permeability function of two different specimens of (i) sheet steel (ii) supermalloy.
The various parameters entering in the representation for the above two specimens are tabulated below:

Table 1

	Sheet Steel	Supermalloy.
$P_1(H)$	$A_1 = 1.000$	$A_1 = 0.400$
	$m_1 = 0.000$ (O.E)	$m_1 = 0.000$ (A.T)
	$\sigma_1 = 0.708$	$\sigma_1 = 0.905$
$P_2(H)$	$A_2 = 1.000$	$A_2 = 0.400$
	$m_2 = 1.000$	$m_2 = 1.450$
	$\sigma_2 = 0.332$	$\sigma_2 = 0.270$
$P_3(H)$	$A_3 = 1.000$	$A_3 = 0.400$
	$m_3 = 1.359$	$m_3 = 2.053$
	$\sigma_3 = 0.745$	$\sigma_3 = 1.1605$
	$H_m = 1.000$	$H_m = 1.700$

The results of this analysis are presented in graphical form in Figures 2.7 and 2.8.

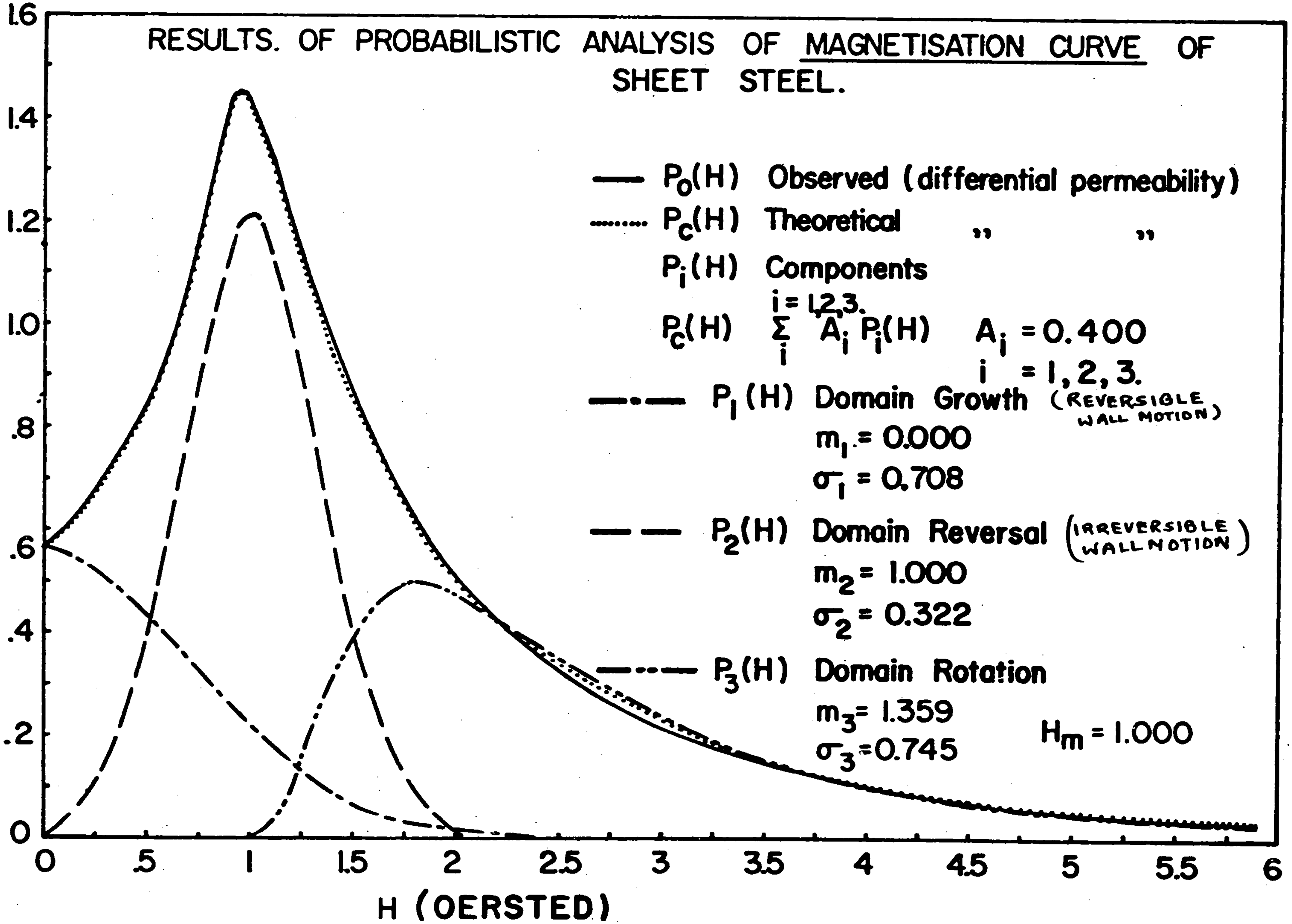
RESULTS. OF PROBABILISTIC ANALYSIS OF MAGNETISATION CURVE OF SHEET STEEL.
P0(H) Observed (differential permeability)
Pc(H) Theoretical " "
Pi(H) Components
Pc(H) Σ Ai Pi(H) i = 1,2,3.
Ai = 0.400
i = 1, 2, 3.
P1(H) Domain Growth (REVERSIBLE WALL MOTION)
m1 = 0.000
σ1 = 0.708
P2(H) Domain Reversal (IRREVERSIBLE WALL MOTION)
m2 = 1.000
σ2 = 0.322
P3(H) Domain Rotation
m3 = 1.359
σ3 = 0.745
Hm = 1.000
2.5 P (H)
1.6
1.4
1.2
1.0
.8
.6
.4
.2
0
.5
1
1.5
2
2.5
3
3.5
4
4.5
5
5.5
6
H (OERSTED)

Fig. 2.7

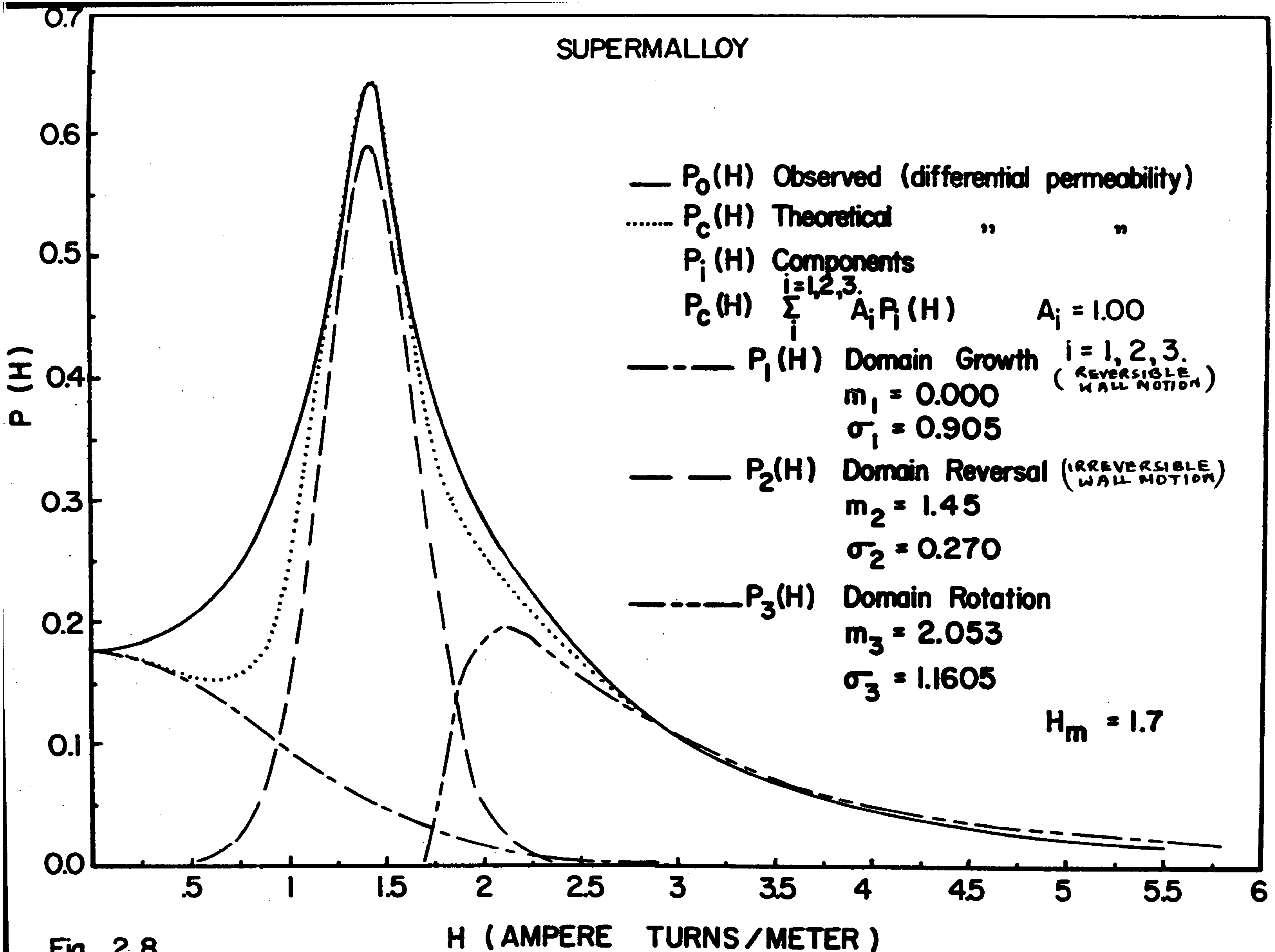
SUPERMALLOY
P (H)
0.0
0.1
0.2
0.3
0.4
0.5
0.6
0.7
.5
1
1.5
2
2.5
3
3.5
4
4.5
5
5.5
6
H (AMPERE TURNS/METER)
P0(H) Observed (differential permeability)
Pc(H) Theoretical " "
Pi(H) Components
Pc(H) Σ i=1,2,3. AiPi(H) Ai = 1.00
P1(H) Domain Growth i = 1, 2, 3. (REVERSIBLE WALL MOTION)
m1 = 0.000
σ1 = 0.905
P2(H) Domain Reversal (IRREVERSIBLE WALL MOTION)
m2 = 1.45
σ2 = 0.270
P3(H) Domain Rotation
m3 = 2.053
σ3 = 1.1605
Hm = 1.7

Fig. 2.8

These results indicate that:

(a) Magnetization by reversible wall motion takes place at relatively low field strength and is predominant in this region,

(b) Magnetization by irreversible wall motion is pronounced in the region of intermediate field strength.

(c) Magnetization through the process of domain rotation always requires a minimum field strength to start with. In high fields magnetization takes place predominantly by domain rotation.

(d) In both the examples, it is observed that though reversible wall motion is predominant in the low field region, it can still take place even after domain rotation has started. Overlapping between the various processes of magnetization is not unlikely.

(e) In these particular examples it is observed that magnetization by irreversible wall motion extends only over a small region and is more predominant as compared to the other two processes.

2.6 An Explanation of Overlapping between the Three Processes of Magnetization.

The reason for overlapping between the three processes of magnetization can be explained as follows:-

In the figure 2.6 it is shown that at the end of every Barkhausen jump magnetization can take place by reversible wall motion as indicated by the arrow segments. This explains the reason for overlapping between reversible wall motion and the two other processes. Overlapping between irreversible wall motion and domain rotation may be due to the presence of some very steep energy peaks which creates obstacles to the motion of walls, unless the applied magnetic field is sufficiently high. But the field already applied may be sufficiently high to cause domain rotation. Such large energy peaks may arise from the presence of impurities.

2.7 Classification of Magnetic Specimens Based on the Above Mathematical Model.

According to the mathematical model presented it is possible to classify magnetic specimens into three main classes: A, B, C. This classification, though somewhat arbitrary, indicates what possible magnetization curves can be represented by the above model.

Class A.

In this class, magnetization takes place by all the three fundamental processes and the total differential permeability function is represented by equation 2.2,

$$P_o(H) = \sum_{i=1}^{3} A_i P_i(H) \qquad A_i \neq 0, i = 1, 2, 3,$$

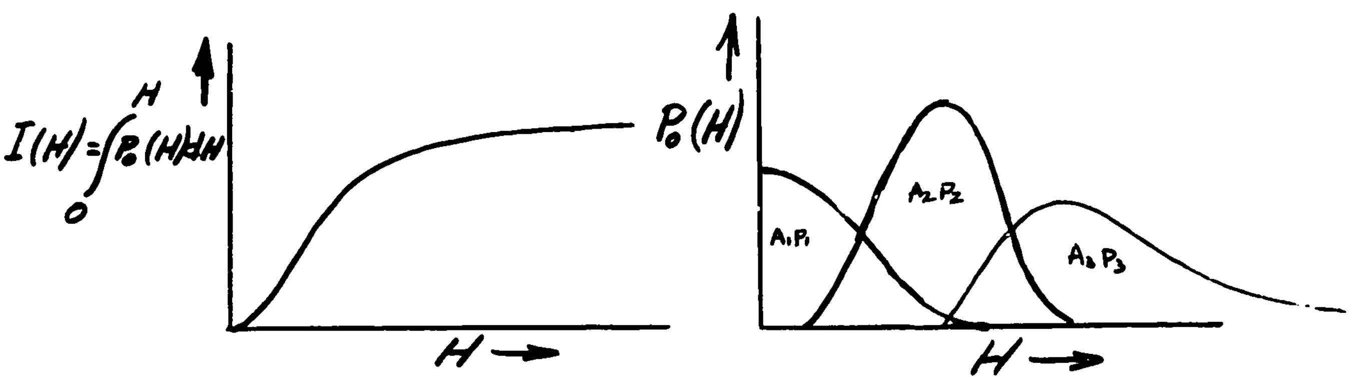

Fig. 2.9a and 2.9b: Class A.

Class B.

Magnetic specimens belonging to class B are magnetized by any two of the three processes. Clearly, there are three subclasses: B_1, B_2, and B_3.

B_1: In this subclass, magnetization is due primarily to reversible and irreversible wall motion, domain rotation being completely suppressed. Thus,

$$P_o(H) = A_1P_1(H) + A_2 P_2(H) \tag{2.6}$$

This situation may arise in slightly impure but highly homogeneous materials. Expected analysis of this subclass of specimens is shown in the Figures 2.10a and 2.10b.

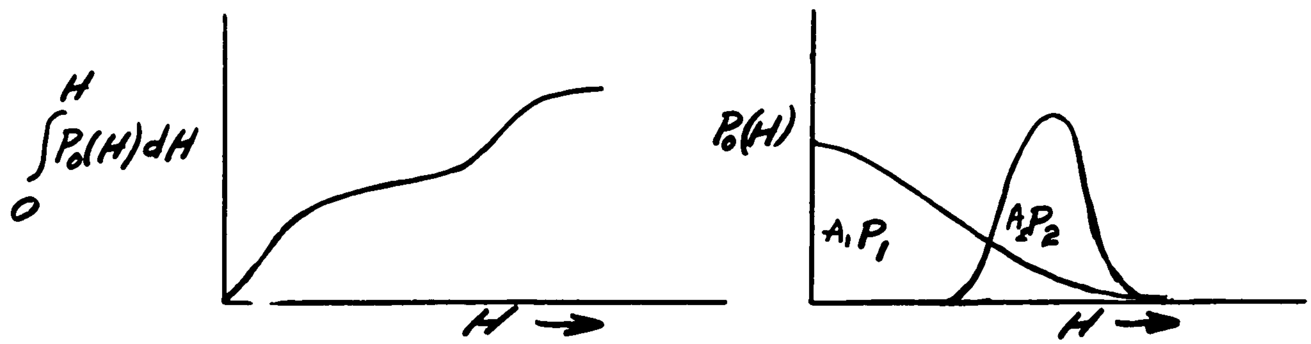

Fig. 2.10a, 2.10b: Class B_1.

B_2: In this subclass magnetization is primarily due to reversible wall motion and domain rotation. Irreversible wall motion may be suppressed by making the material highly pure and heterogeneous. In this case the differential permeability function is expressed as

$$P_o(H) = A_1P_1(H) + A_3P_3(H) \tag{2.7}$$

Expected result of analysis of this subclass of magnetic specimens is shown in Figures, 2.11a and 2.11b.

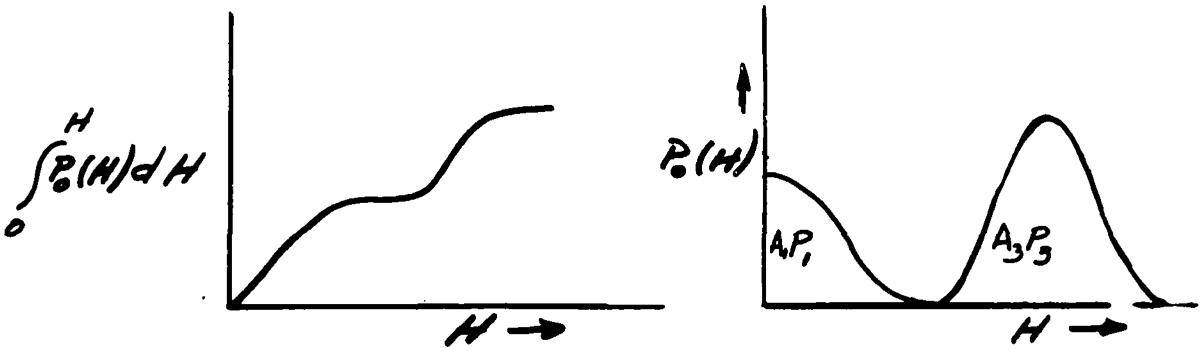

Fig. 2.11a, 2.11b: Class B_2

B_3: In this subclass magnetization takes place by irreversible wall motion and domain rotation. Magnetization by reversible wall motion is suppressed. The corresponding $P_o(H)$ is given by,

$$P_o(H) = A_2P_2(H) + A_3P_3(H). \quad (2.8)$$

This situation may be expected to occur in highly impure materials with heterogeneous structure. This is illustrated in Figures 2.12a, 2.12b.

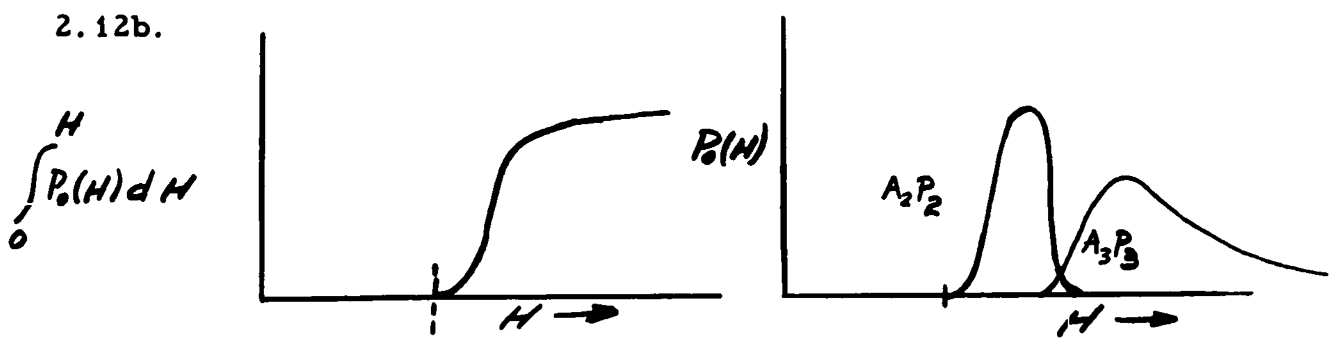

Fig. 2.12a, 2.12b: Class B_3.

Class C.

Magnetic specimens belonging to class C are magnetized by any one of three fundamental processes of magnetization. Clearly, there are three subclasses C_1, C_2, and C_3.

C_1: In this subclass magnetization takes place through the process of reversible boundary displacement alone. Thus

$$P_o(H) = A_1P_1(H). \tag{2.9}$$

This situation may be expected to arise in homogeneous materials of very high degree of purity. The expected result of analysis is shown in the Figures 2.13a, 2.13b.

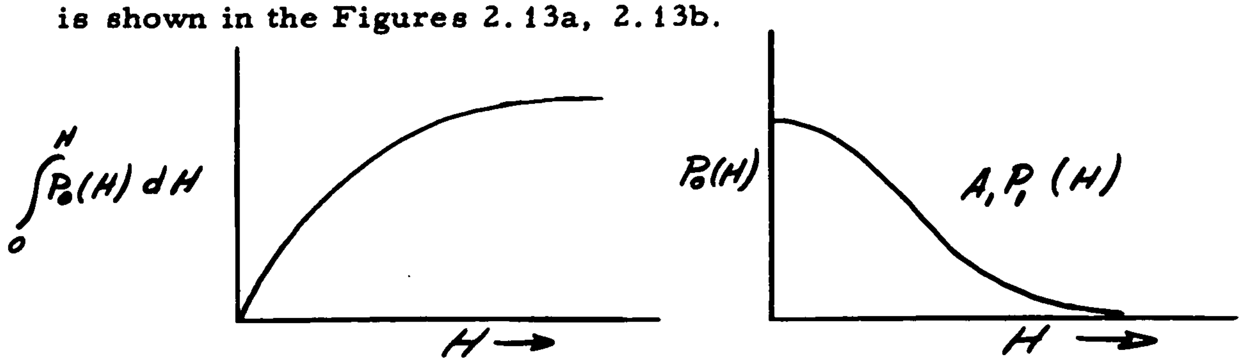

Fig. 2.13a, 2.13b: Class C_1.

C_2: In this subclass magnetization takes place primarily by irreversible boundary displacement.

Thus, $$P_o(H) = A_2P_2(H). \tag{2.10}$$

This situation may be expected to occur in very impure but homogeneous materials. Expected result of analysis of this subclass of magnetic specimens is shown in the Figures 2.14a and 2.14b.

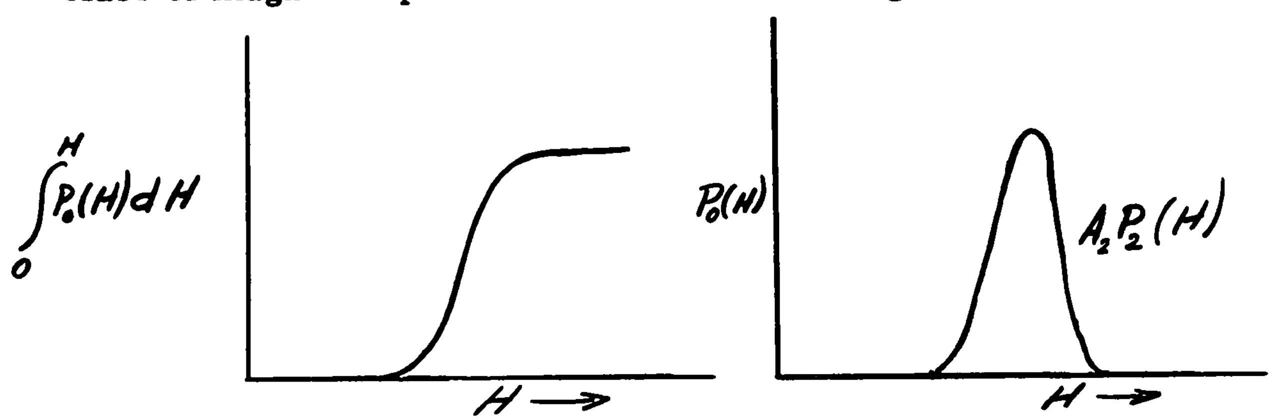

Fig. 2.14a, 2.14b: Class C_2.

C_3: Magnetization by domain rotation alone, can occur in specimens where domain walls do not exist. This situation may arise in powder cores where the grains may be so small that domain wall formation is energetically unfavorable. In this case,

$$P_o(H) = A_3 P_3(H). \tag{2.11}$$

Expected result of analysis of such specimens are shown in the Figures 2.15a and 2.15b.

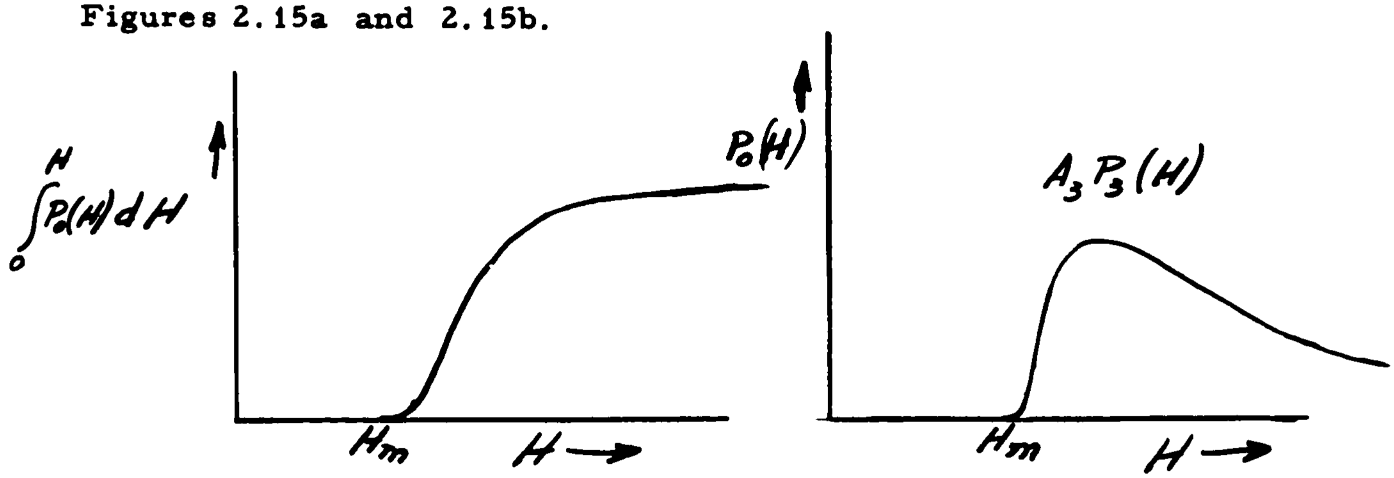

Fig. 2.15a, 2.15b: Class C_3.

2.8 Hysteresis Loops.

In this case essentially, the same mathematical model is applied. An extra term is added to take account of domain rotation in reverse field. The function $P_o(H)$ is obtained from the first derivative of one of the arms of the hysteresis loop and $P_o(H)$ is expressed as,

$$P_o(H) = \sum_{i=1}^{4} A_i P_i(H) \tag{2.12}$$

where

$$P_1(H) = \frac{1}{\sigma_1\sqrt{2\pi}\,(-H+Hm_1)} \exp -\frac{1}{2}\left[\frac{(\log(-H+Hm_1)-m_1)^2}{\sigma_1^2}\right] \tag{2.13}$$

$$P_2(H) = \frac{1}{\sigma_2\sqrt{2\pi}} \exp -\frac{1}{2}\left[\frac{(H-m_2)^2}{\sigma_2^2}\right] \tag{2.14}$$

$$P_3(H) = \frac{1}{\sigma_3\sqrt{2\pi}} \exp - \frac{1}{2} \left[\frac{(H-m_3)^2}{\sigma_3^2} \right] \tag{2.15}$$

and,

$$P_4(H) = \frac{1}{\sigma_4 \sqrt{2\pi}\,(H-Hm_4)} \exp - \frac{1}{2} \left[\frac{(\log(H-Hm_4)-m_4)^2}{\sigma_4^2} \right] \tag{2.16}$$

The symbols σ_i^2, m_i and H_{m_i} are the variances, means and the starting fields respectively for the i-th process. The functions p_1 and p_4 represent domain rotation in the presence of high negative and positive fields respectively. The functions p_2 and p_3 represent reversible and irreversible wall motion respectively. The expression, equation 2.12, is used to represent the differential permeability function obtained from any one of the arms of hysteresis loop. In case of symmetric hysteresis loops the differential permeability function corresponding to the other arm of the hysteresis loop is easily obtained by a mirror image reflection of $p_o(H)$ around H = 0. The order of occurence of the three basic processes of magnetization are shown on the hysteresis loop, Figure 2.16.

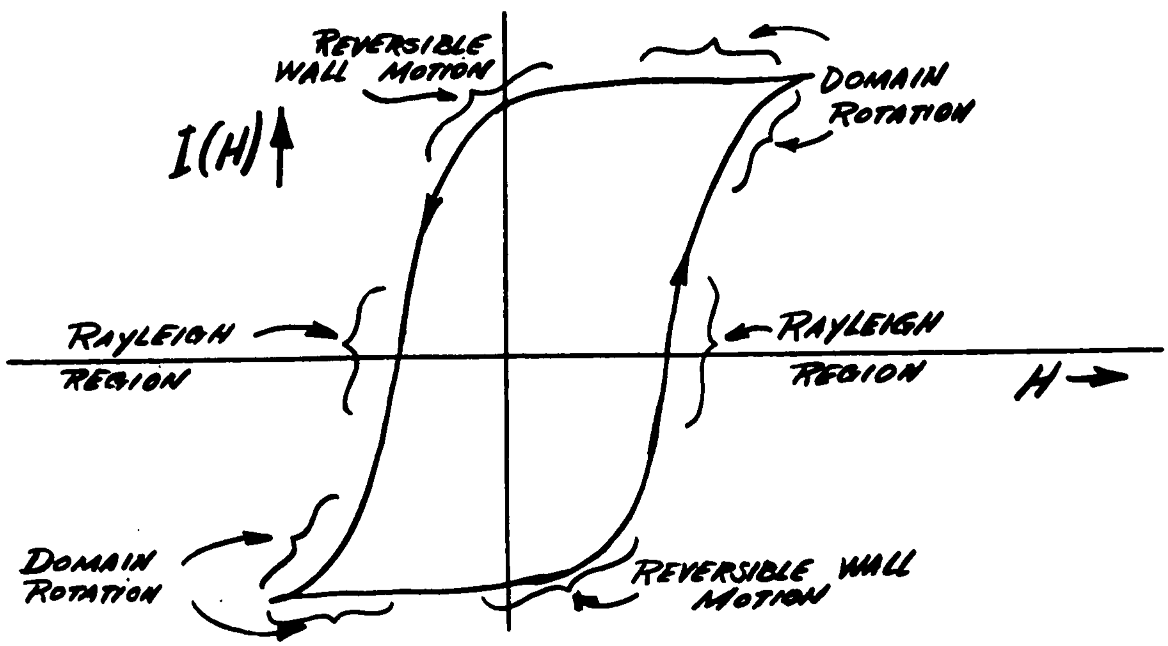

Fig. 2.16 Interpretation of Hysteresis Loops.

This model has been successfully applied to hysteresis loops of hot rolled steel sheets, u. s. s. transformer, 72 - 26 gage. The values of the various parameters entering in the representation are tabulated below, and the results are presented in graphical form in Figure 2.17.

Table 2

$$A_1 = A_2 = A_3 = A_4 = 7.250$$

Name of the Process	Symbol used	m_i o.e	σ_i	H_{m_i} o.e
Domain rotation	$P_1(H)$	1.945	1.060	-0.371
Reversible wall motion	$P_2(H)$	0.380	0.700	-
Irreversible wall motion	$P_3(H)$	0.590	0.169	-
Domain rotation	$P_4(H)$	0.680	1.140	+0.375

It is interesting to note that the magnitudes of the starting field for domain rotation is approximately the same in either direction of the applied field. This appears to suggest that the process of domain rotation is independent of the direction of the applied field and hence the state of magnetization.

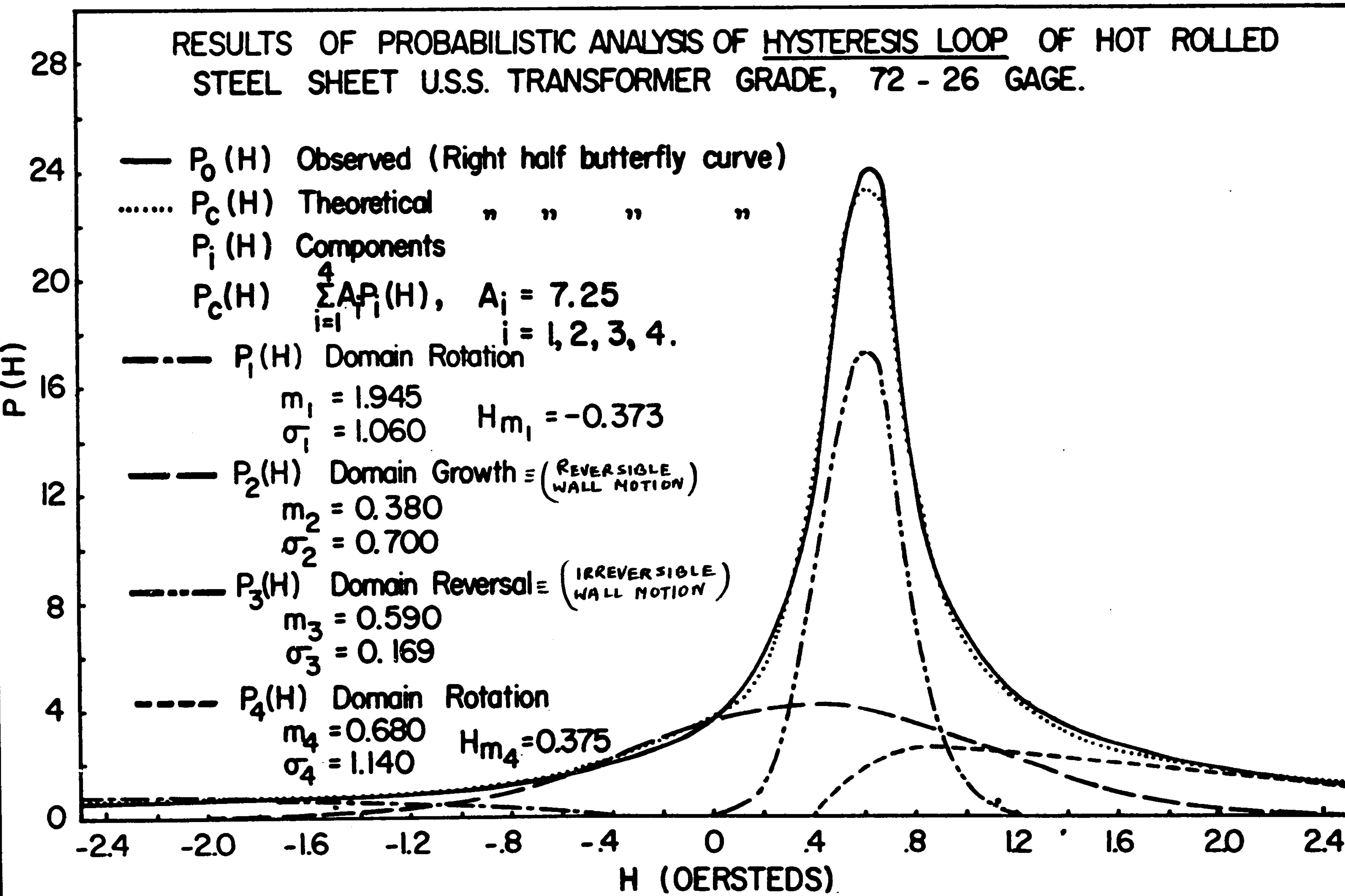
RESULTS OF PROBABILISTIC ANALYSIS OF HYSTERESIS LOOP OF HOT ROLLED STEEL SHEET U.S.S. TRANSFORMER GRADE, 72 - 26 GAGE.
P₀(H) Observed (Right half butterfly curve)
Pc(H) Theoretical " " " "
Pi(H) Components
Pc(H) ΣAiPi(H), Ai = 7.25, i = 1, 2, 3, 4.
P1(H) Domain Rotation
m1 = 1.945
σ1 = 1.060
Hm1 = -0.373
P2(H) Domain Growth ≡ (REVERSIBLE WALL MOTION)
m2 = 0.380
σ2 = 0.700
P3(H) Domain Reversal ≡ (IRREVERSIBLE WALL MOTION)
m3 = 0.590
σ3 = 0.169
P4(H) Domain Rotation
m4 = 0.680
σ4 = 1.140
Hm4 = 0.375
P(H)
H (OERSTEDS)

Fig. 2.17

2.9 Square Hysteresis Loops.

In the case of square hysteresis loop, the mathematical model presented may still remain valid. If the square loop is assumed to be due to anyone of the three processes of magnetization, for example, the ith process, then the function

$$P_o(H) = A_i \, \delta(H - H_i) \; ; \qquad (2.17)$$

where A_i is the strength of the impulse. In this situation, I(H) is given by,

$$I(H) = I(-\infty) + \int_{-\infty}^{H} P_o(H)dH$$

$$= -I_s + \int_{-\infty}^{H} A_i \, \delta(H - H_i) \, dH$$

$$= -I_s + A_i \qquad (2.18)$$

But $A_i = 2I_s$ Hence

$$I(H) = I_s \quad \text{for } H \geqslant H_i$$

where I_s is the saturation magnetization.

The value of H_i depends on the process of magnetization involved. If the magnetization is due only to irreversible wall motion, $H_i = m_3$ and

$$P_o(H) = A_3 \, \delta(H-m_3) \qquad (2.19)$$

and $A_3 = 2I_s$, $A_1 = A_2 = A_4 = 0$.

If the magnetization is due to domain rotation only then, $P_o(H)$ is given by the following expression:

$$P_o(H) = A_1 \, \delta[H-(-H_{m_1} + e^{-m_1})] + A_4 \, \delta[H-(H_{m4} + e^{m_4})] \quad (2.20)$$

If the loop is perfectly rectangular then, $-H_{m_1} = H_{m_4}$ and $-m_1 = m_4$ and

$$P_o(H) = (A_1+A_4)\,\delta\,[H-(-H_{m_4}+e^{m_4})]$$

$$A_1 + A_4 = 2I_s\ ,\quad A_2 = A_3 = 0.$$

The most interesting case is one, in which $-H_{m_1} + e^{-m_1} \neq H_{m_4} + e^{m_4}$.

In this case the hysteresis loop takes a very peculiar form as shown in Figure 2.17A.

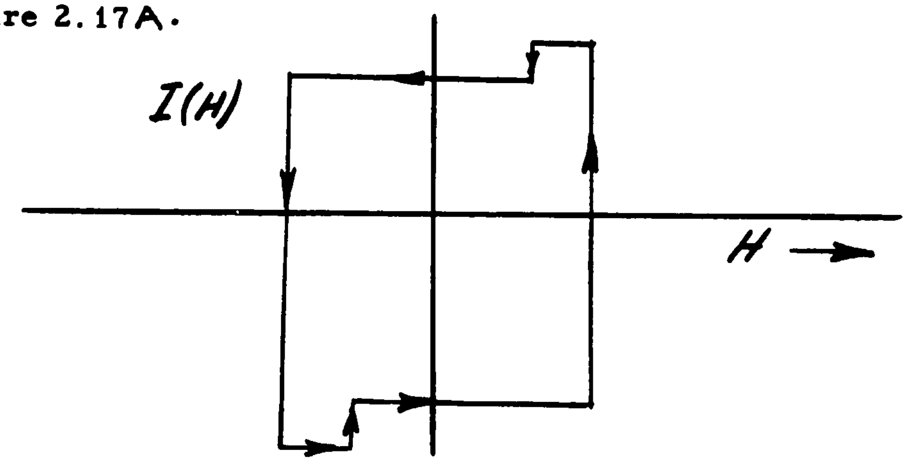

Fig. 2.17A: Ideal Hysteresis Loop of Perminvar Alloys.

This type of hysteresis loop is rare, but may be observed in perminvar alloys (Ref. 6, pp. 173).

CONCLUSION

(i) In conclusion it must be stated that the representation of magnetization processes as developed here is not the only possible one, because these processes can be more accurately represented by the well known Gram Charlier series. But the advantage of the representation presented here lies in the simplicity of its form. Moreover it utilizes the concepts of the basic processes of magnetization as provided by domain theory of magnetism.

(II) In this representation $P_o(H) = \sum_{i=1} A_i P_i(H)$ yields the total differential permeability as a function of field strength H. Such a functional relationship may be useful in the design of certain magnetic devices.

(iii) Since the expression for total differential permeability is presented as a sum of appropriately weighted probability functions, one may consider the process of magnetization of polycrystalline specimens as a probabilistic phenomenon.

(iv) In this work only quasi static magnetization curves and hysteresis loops were considered; it is questionable if this representation would be valid for dynamic magnetization processes.

(v) It is natural in the process of magnetization to consider the statistical parameters, σ's, m's and Hm_i' s as functions of the following physical parameters:

C = concentration of alloying materials

α = externally applied stress

T = temperature of the specimen

H'm= maximum input signal amplitude

ω = frequency of the input signal.

i.e.

$$\sigma_i = \sigma_i(c, \alpha, T, H'_m, \omega)$$
$$m_i = m_i(c, \alpha, T, H'_m, \omega) \quad (2.21)$$
$$H_{m_i} = H_{m_i}(c, \alpha, T, H'_m, \omega)$$

If such functional relationships exist and if the representation provided in this work is valid for the dynamic case, then the magnetic behavior of a magnetic specimen under most of the situations can be approximately predicted by our representation. If we consider c, α, and T to be fixed, then the problem is further simplified and the equations 2.21 reduce to the form,

$$\sigma_i = \sigma_i (H'_m, \omega)$$
$$m_i = m_i (H'_m, \omega) \quad (2.22)$$
$$H_{m_i} = H_{m_i} (H'_m, \omega)$$

and $P_i(H)$ can be considered as a function of σ_i, m_i, H_{m_i} in addition to H.

i.e., $P_i(H; \sigma_i, m_i, H m_i)$

$$= P_i[H; \sigma_i(H'_m, \omega), m_i(H'_m, \omega); H_{m_i}(H'_m, \omega)] \quad (2.23)$$

and

$$P_o(H) = \sum_{i=1} A_i P_i (H, \sigma_i, m_i, H_{m_i}) \quad (2.24)$$

If such relations can be established, and the above representation is proved valid then it is clear that one obtains a family of hysteresis loops. Each member of this family corresponds to either a specific value of the maximum input signal amplitude H'_{m_k} for constant ω Fig. 2.18 or to a specific value of ω_k for constant H'_m Fig. 2.19.

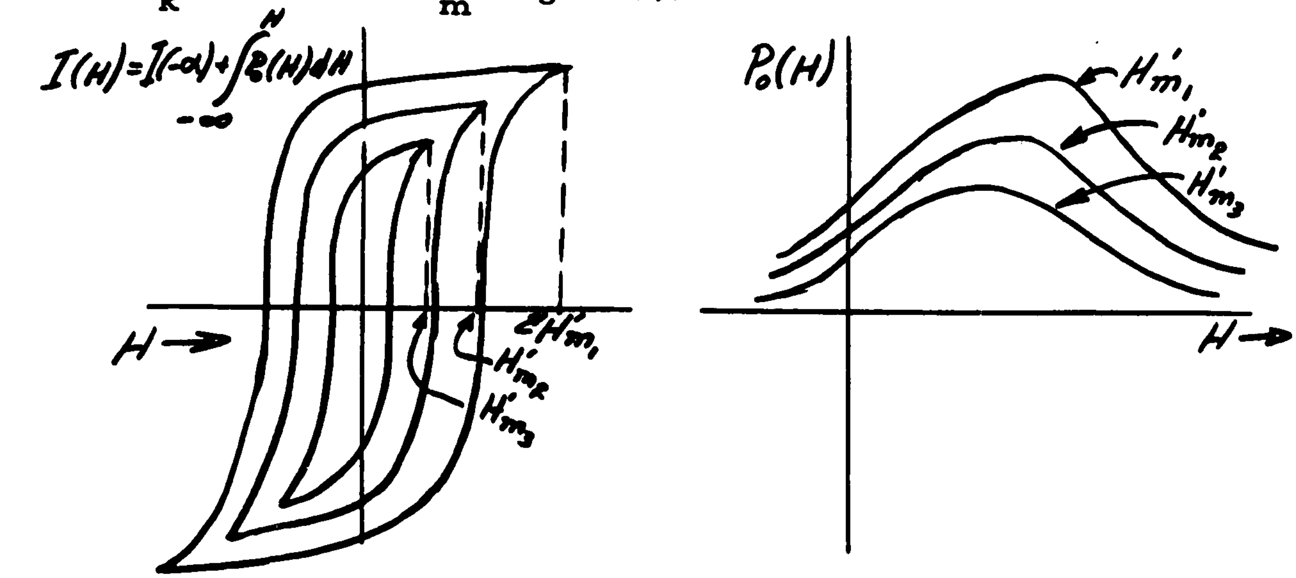

Fig. 2.18: Constant ω, variable H'_m.

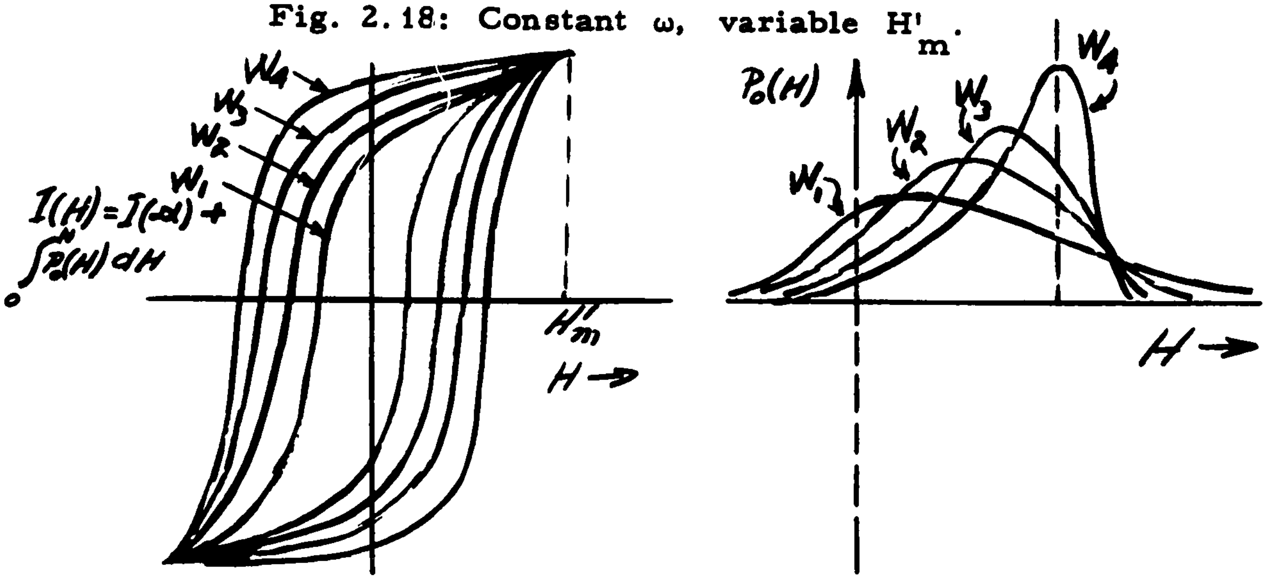

Fig. 2.19: Constant H'_m and variable ω .

There are two areas of further development of this work.

(i) To develop some technique for the detection of the processes of magnetization and show that the results produced correspond to actual physical reality.

(ii) To establish the functional relationships as in equations 2.22, if there exist any.

APPENDIX A
COMPUTATIONS.

A1. Method I

The function $P_o(H)$ with $H \in I$, is sought to be represented by a sum of terms of the form $\sum_{i=1}^{3} A_i P_i(H)$, where $P_i(H)$ (i = 1, 2, 3) are as defined in equations 2.3, 2.4 and 2.5. The problem is to choose the set $\{A_i\}_{i=1}^{3}$, $\{m_i\}_{i=1}^{3}$, $\{\sigma_i\}_{i=1}^{3}$ and H_m such that

$$E = \sum_{k=1}^{n} \left[P_o(H_k) - \sum_{i=1}^{3} A_i P_i(H_k) \right]^2 \qquad \text{(A1.1)}$$

is a minimum, where n is a suitable number of subintervals into which the domain I of the function $P_o(H)$ is divided. This is the well known least square approximation which can be performed as follows:

$P_o(H)$ is written explicity as a function of all the relevant parameters including the variable H. Thus

$$P_o(H) = f(A_1, A_2, A_3; m_1, m_2, m_3; \sigma_1, \sigma_2, \sigma_3; H_m; H) \qquad \text{(A1.2)}$$

which can be more conveniently written as $P_o(H) = f(s, H)$ where s is defined as a point in the n-space. That is $s \triangleq (A_1, A_2, A_3; m_1, m_2, m_3, \sigma_1, \sigma_2, \sigma_3; H_m)$ with n = 10. Assuming an approximate value for s the function f(s, H) can be expanded in multidimensional Taylor's series about the point $s = s_o \triangleq (A_{1_o}\ A_{2_o}\ A_{3_o};\ m_{1_o}\ m_{2_o}\ m_{3_o} \ldots H_{m_o})$

provided it is continuous with respect to s and derivatives of all orders exist for each $H \in I$. These conditions are usually satisfied for the specific problem under consideration and f can be expanded as follows:

$$f(s,H) = \sum_{i_1=o}^{\infty} \cdots \sum_{i_{10}=o}^{\infty} \frac{1}{i_1! \cdots i_{10}!} \frac{\partial^{i_1+i_2+\cdots+i_{10}} f(s,H)}{\partial A_1^{i_1} \cdots \partial H_m^{i_{10}}} \Bigg|_{s=s_o} (\Delta A_1)^{i_1} \cdots (\Delta H_m)^{i_{10}} \quad \text{(A1.3)}$$

where $S = s_o + \Delta s$ and

$$\Delta s = (\Delta A_1, \Delta A_2, \Delta A_3; \ \Delta m_1, \Delta m_2, \Delta m_3, \Delta\sigma_1, \Delta\sigma_2 \ \Delta\sigma_3, \Delta H_m)$$

If the initially chosen value for the point s as s_o is close to the true value of s then all terms of order higher than the first can be neglected and the residuals for each value of $H \in I$ can be calculated. Denoting residuals by r(H) for each $H \in I$, the residual equation can be written as

$$r(H) = f_c(s_o, H) - f_o(s,H) + \sum_{i=1}^{3} \frac{\partial f}{\partial A_i}\Bigg|_{s=s_o} (\Delta A_i) + \sum_{i=1}^{3} \frac{\partial f}{\partial m_i}\Bigg|_{s=s_o} (\Delta m_i)$$

$$+ \sum_{i=1}^{3} \frac{\partial f}{\partial \sigma_i}\Bigg|_{s=s_o} (\Delta\sigma_i) + \frac{\partial f}{\partial H_m}\Bigg|_{s=s_o} (\Delta H_m) \quad \text{(A1.4)}$$

where f_c is the calculated value of f(s, H) at $s = s_o$ and $f_o(s,H)$ is the corresponding observed value of $P_o(H)$. Let $\{r(H_k)\}_{k=1}^{n}$ be the values of the function r(H) and let $E = \sum_{k=1}^{n} \left[r(H_k)\right]^2$. It is clear that E is a function of $\Delta s = (\Delta A_1, \ldots \Delta H_m)$, which must be chosen such that E is a minimum.

This is obtained by setting the derivative of E with respect to Δs equal to zero, and solving the resulting algebraic equations for the unknown. One of the ten equations is shown below.

$$\sum_{k=1}^{n} \left(\frac{\partial f}{\partial A_1}\right)^2 \Delta A_1 + \sum_{k=1}^{n} \left(\frac{\partial f}{\partial A_1}\right)\left(\frac{\partial f}{\partial A_2}\right) \Delta A_2 + \sum_{k=1}^{n} \left(\frac{\partial f}{\partial A_1}\right)\left(\frac{\partial f}{\partial A_3}\right) \Delta A_3$$

$$+ \sum_{k=1}^{n} \left(\frac{\partial f}{\partial A_1}\right)\left(\frac{\partial f}{\partial m_1}\right) \Delta m_1 + \sum_{k=1}^{n} \left(\frac{\partial f}{\partial A_1}\right)\left(\frac{\partial f}{\partial m_2}\right) \Delta m_2 + \sum_{k=1}^{n} \left(\frac{\partial f}{\partial A_1}\right)\left(\frac{\partial f}{\partial m_3}\right) \Delta m_3$$

$$+ \sum_{k=1}^{n} \left(\frac{\partial f}{\partial A_1}\right)\left(\frac{\partial f}{\partial \sigma_1}\right) \Delta \sigma_1 + \sum_{k=1}^{n} \left(\frac{\partial f}{\partial A_1}\right)\left(\frac{\partial f}{\partial \sigma_2}\right) \Delta \sigma_2 + \sum_{k=1}^{n} \left(\frac{\partial f}{\partial A_1}\right)\left(\frac{\partial f}{\partial \sigma_3}\right) \Delta \sigma_3$$

$$+ \sum_{k=1}^{n} \left(\frac{\partial f}{\partial A_1}\right)\left(\frac{\partial f}{\partial H_m}\right) \Delta H_m = \sum_{k=1}^{n} (f_o - f_c) \frac{\partial f}{\partial A_1} \qquad \text{(A1.5)}$$

Exactly the same procedure is followed in the case of hysteresis loop analysis. In this case the function $P_o(H)$ is given by the equation 2.12. In order to reduce the dimensionality, A_i's are all chosen equal and $P_o(H)$ is written explicitly as $P_o(H) = f(A, \sigma_1, m_1, a_1; \sigma_2, m_2; \sigma_3, m_3; \sigma_4, m_4, a_4, H)$ where $A_1 = A_2 = A_3 = A_4 \triangleq A$, $H_{m_1} \triangleq a_1$ and $H_{m_4} \triangleq a_4$.

By the use of residual equations and the least square method, one obtains eleven algebraic equations in eleven unknowns. This is written in matrix form as shown in Table A_1. The unknowns here, are denoted by c_i ($i = 1, 2, 11$). The matrix formed from the coefficients of these equations is symmetric, therefore only the upper triangle is shown. In this equation $A\underline{C} = \underline{Y}$, the matrix A is known and the vector $\underline{Y}$ is also known, $\underline{C}$ is to be determind.

$\underline{C}$ and $\underline{Y}$ are defined below,

$$\underline{C} = \begin{bmatrix} c_1 \\ \\ c_{11} \end{bmatrix}, \quad \underline{Y} = \begin{bmatrix} Y_1 \\ \\ Y_{11} \end{bmatrix} \quad \text{where}$$

$$\begin{aligned} Y_1 &= \sum_{i=1}^{n} (f_i - f_i') \frac{\partial f_i}{\partial A} , \\ &\cdots\cdots\cdots\cdots \\ Y_{11} &= \sum_{i=1}^{n} (f_i - f_i') \frac{\partial f_i}{\partial a_4} \end{aligned} \qquad (A1.6)$$

and f_i is the observed value of $P_o(H)$ at $H = H_i$ and f_i' is the corresponding calculated value. By solving the algebraic equations, the unknowns can be determined.

A2. Method 2

There is one disadvantage in the above procedure of computation. If the values of the parameters initially chosen are far from their true values then the first order linear approximation does not apply. Higher order terms must be included. To avoid the resulting complexity it is found advisable to keep some provision in the program to automatically adjust the values of the parameters, whenever there is a tendency of divergence .

A direct approach is to choose the values of the parameters from a set of suitable values preassigned to each one of the members of the set and compute

$$E = \sum_{k=1}^{n} \left[f_o(H_k) - f_c(H_k) \right]^2 \qquad (A2.1)$$

TABLE A.1

$$f_i = f\,(A, \sigma_1, m_1, a_1, \sigma_2, m_2, \sigma_3, m_3, a_4, \sigma_4, m_4, x_i)$$

$$\begin{bmatrix}
\sum_{i=1}^{N}\left(\frac{\partial f_i}{\partial A}\right)^2 & \sum\frac{\partial f_i}{\partial \sigma_1}\cdot\frac{\partial f_i}{\partial A} & \sum\frac{\partial f_i}{\partial m_1}\cdot\frac{\partial f_i}{\partial A} & \sum\frac{\partial f_i}{\partial a_1}\cdot\frac{\partial f_i}{\partial A} & \sum\frac{\partial f_i}{\partial \sigma_2}\cdot\frac{\partial f_i}{\partial A} & \sum\frac{\partial f_i}{\partial m_2}\cdot\frac{\partial f_i}{\partial A} & \sum\frac{\partial f_i}{\partial \sigma_3}\cdot\frac{\partial f_i}{\partial A} & \sum\frac{\partial f_i}{\partial m_3}\cdot\frac{\partial f_i}{\partial A} & \sum\frac{\partial f_i}{\partial a_4}\cdot\frac{\partial f_i}{\partial A} & \sum\frac{\partial f_i}{\partial \sigma_4}\cdot\frac{\partial f_i}{\partial A} & \sum\frac{\partial f_i}{\partial m_4}\cdot\frac{\partial f_i}{\partial A} \\
 & \sum\left(\frac{\partial f_i}{\partial \sigma_1}\right)^2 & \sum\frac{\partial f_i}{\partial m_1}\cdot\frac{\partial f_i}{\partial \sigma_1} & \sum\frac{\partial f_i}{\partial a_1}\cdot\frac{\partial f_i}{\partial \sigma_1} & \sum\frac{\partial f_i}{\partial \sigma_2}\cdot\frac{\partial f_i}{\partial \sigma_1} & \sum\frac{\partial f_i}{\partial m_2}\cdot\frac{\partial f_i}{\partial \sigma_1} & \sum\frac{\partial f_i}{\partial \sigma_3}\cdot\frac{\partial f_i}{\partial \sigma_1} & \sum\frac{\partial f_i}{\partial m_3}\cdot\frac{\partial f_i}{\partial \sigma_1} & \sum\frac{\partial f_i}{\partial a_4}\cdot\frac{\partial f_i}{\partial \sigma_1} & \sum\frac{\partial f_i}{\partial \sigma_4}\cdot\frac{\partial f_i}{\partial \sigma_1} & \sum\frac{\partial f_i}{\partial m_4}\cdot\frac{\partial f_i}{\partial \sigma_1} \\
 & & \sum\left(\frac{\partial f_i}{\partial m_1}\right)^2 & \sum\frac{\partial f_i}{\partial a_1}\cdot\frac{\partial f_i}{\partial m_1} & \sum\frac{\partial f_i}{\partial \sigma_2}\cdot\frac{\partial f_i}{\partial m_1} & \sum\frac{\partial f_i}{\partial m_2}\cdot\frac{\partial f_i}{\partial m_1} & \sum\frac{\partial f_i}{\partial \sigma_3}\cdot\frac{\partial f_i}{\partial m_1} & \sum\frac{\partial f_i}{\partial m_3}\cdot\frac{\partial f_i}{\partial m_1} & \sum\frac{\partial f_i}{\partial a_4}\cdot\frac{\partial f_i}{\partial m_1} & \sum\frac{\partial f_i}{\partial \sigma_4}\cdot\frac{\partial f_i}{\partial m_1} & \sum\frac{\partial f_i}{\partial m_4}\cdot\frac{\partial f_i}{\partial m_1} \\
 & & & \sum\left(\frac{\partial f_i}{\partial a_1}\right)^2 & \sum\frac{\partial f_i}{\partial \sigma_2}\cdot\frac{\partial f_i}{\partial a_1} & \sum\frac{\partial f_i}{\partial m_2}\cdot\frac{\partial f_i}{\partial a_1} & \sum\frac{\partial f_i}{\partial \sigma_3}\cdot\frac{\partial f_i}{\partial a_1} & \sum\frac{\partial f_i}{\partial m_3}\cdot\frac{\partial f_i}{\partial a_1} & \sum\frac{\partial f_i}{\partial a_4}\cdot\frac{\partial f_i}{\partial a_1} & \sum\frac{\partial f_i}{\partial \sigma_4}\cdot\frac{\partial f_i}{\partial a_1} & \sum\frac{\partial f_i}{\partial m_4}\cdot\frac{\partial f_i}{\partial a_1} \\
 & & & & \sum\left(\frac{\partial f_i}{\partial \sigma_2}\right)^2 & \sum\frac{\partial f_i}{\partial m_2}\cdot\frac{\partial f_i}{\partial \sigma_2} & \sum\frac{\partial f_i}{\partial \sigma_3}\cdot\frac{\partial f_i}{\partial \sigma_2} & \sum\frac{\partial f_i}{\partial m_3}\cdot\frac{\partial f_i}{\partial \sigma_2} & \sum\frac{\partial f_i}{\partial a_4}\cdot\frac{\partial f_i}{\partial \sigma_2} & \sum\frac{\partial f_i}{\partial \sigma_4}\cdot\frac{\partial f_i}{\partial \sigma_2} & \sum\frac{\partial f_i}{\partial m_4}\cdot\frac{\partial f_i}{\partial \sigma_2} \\
 & & & & & \sum\left(\frac{\partial f_i}{\partial m_2}\right)^2 & \sum\frac{\partial f_i}{\partial \sigma_3}\cdot\frac{\partial f_i}{\partial m_2} & \sum\frac{\partial f_i}{\partial m_3}\cdot\frac{\partial f_i}{\partial m_2} & \sum\frac{\partial f_i}{\partial a_4}\cdot\frac{\partial f_i}{\partial m_2} & \sum\frac{\partial f_i}{\partial \sigma_4}\cdot\frac{\partial f_i}{\partial m_2} & \sum\frac{\partial f_i}{\partial m_4}\cdot\frac{\partial f_i}{\partial m_2} \\
 & & & & & & \sum\left(\frac{\partial f_i}{\partial \sigma_3}\right)^2 & \sum\frac{\partial f_i}{\partial m_3}\cdot\frac{\partial f_i}{\partial \sigma_3} & \sum\frac{\partial f_i}{\partial a_4}\cdot\frac{\partial f_i}{\partial \sigma_3} & \sum\frac{\partial f_i}{\partial \sigma_4}\cdot\frac{\partial f_i}{\partial \sigma_3} & \sum\frac{\partial f_i}{\partial m_4}\cdot\frac{\partial f_i}{\partial \sigma_3} \\
 & & & & & & & \sum\left(\frac{\partial f_i}{\partial m_3}\right)^2 & \sum\frac{\partial f_i}{\partial a_4}\cdot\frac{\partial f_i}{\partial m_3} & \sum\frac{\partial f_i}{\partial \sigma_4}\cdot\frac{\partial f_i}{\partial m_3} & \sum\frac{\partial f_i}{\partial m_4}\cdot\frac{\partial f_i}{\partial m_3} \\
 & & & & & & & & \sum\left(\frac{\partial f_i}{\partial a_4}\right)^2 & \sum\frac{\partial f_i}{\partial \sigma_4}\cdot\frac{\partial f_i}{\partial a_4} & \sum\frac{\partial f_i}{\partial m_4}\cdot\frac{\partial f_i}{\partial a_4} \\
 & & & & & & & & & \sum\left(\frac{\partial f_i}{\partial \sigma_4}\right)^2 & \sum\frac{\partial f_i}{\partial m_4}\cdot\frac{\partial f_i}{\partial \sigma_4} \\
 & & & & & & & & & & \sum\left(\frac{\partial f_i}{\partial m_4}\right)^2
\end{bmatrix}
\begin{bmatrix} C_1 \\ C_2 \\ C_3 \\ C_4 \\ C_5 \\ C_6 \\ C_7 \\ C_8 \\ C_9 \\ C_{10} \\ C_{11} \end{bmatrix}
=
\begin{bmatrix}
\sum (y_i - y_i')\frac{\partial f_i}{\partial A} \\
\sum (y_i - y_i')\frac{\partial f_i}{\partial \sigma_1} \\
\sum (y_i - y_i')\frac{\partial f_i}{\partial m_1} \\
\sum (y_i - y_i')\frac{\partial f_i}{\partial a_1} \\
\sum (y_i - y_i')\frac{\partial f_i}{\partial \sigma_2} \\
\sum (y_i - y_i')\frac{\partial f_i}{\partial m_2} \\
\sum (y_i - y_i')\frac{\partial f_i}{\partial \sigma_3} \\
\sum (y_i - y_i')\frac{\partial f_i}{\partial m_3} \\
\sum (y_i - y_i')\frac{\partial f_i}{\partial a_4} \\
\sum (y_i - y_i')\frac{\partial f_i}{\partial \sigma_4} \\
\sum (y_i - y_i')\frac{\partial f_i}{\partial m_4}
\end{bmatrix}$$

$A\underline{C} = \underline{Y}$

Since $A^T = A$ the lower triangle of the matrix is omitted.

$\underline{C} = A^{-1}\underline{Y}$ is desired.

$N = 34$ number of observational data.

C_j ($j = 1, 2, \ldots, 11$) are the correction terms to be added to $A_0\sigma_{10}m_{10}a_{10}\sigma_{20}m_{20}\sigma_{30}m_{30}a_{40}\sigma_{40}m_{40}$ respectively to obtain the correct values. 0's are used as additional subscripts to indicate that these are initially chosen values.

$\begin{bmatrix} y_1' \\ \vdots \\ y_N' \end{bmatrix}$, are the calculated values of f from the assumed values of the parameters.

$\begin{bmatrix} y_1 \\ \vdots \\ y_N \end{bmatrix}$ are the experimental data for 'f' where $f_o(H_k)$ is the observed value of the function $P_o(H)$ at $H = H_k$ and $f_c(H_k)$ is the calculated value of the function $P_o(H)$ at $H = H_k$, and for a suitable subset of values of the parameters taken one for each from its preassigned set. If ten possible values are chosen for each of ten unknowns, then it is necessary to compute 10^{10} values of E and choose the minimum. This appears to be laborious, but in actual practice it is not necessary to compute such large number of values. Since the parameters are mutually independent, it is possible to fix nine out of ten parameters and let the 10th one assume all possible values preassigned to it and find the corresponding minimum for E and fix this value of the tenth parameter. This can be repeated for each of the parameters and the final minimum in E is determined and the corresponding values of the parameters give the closest approximation to their true values. In this case only 10^2 trials are necessary. This can be further improved by making proper decision during the process of computation by cutting down the length of the set of values preassigned to each of the unknown parameters.

Both these methods have been used in the computation. Sometime it is advantageous to use the second method first and obtain a set of approximate values of the parameters to be estimated and then apply the first method to improve the accuracy of the results.

A3. Computer Results.

Complete computer results are available in the departmental files. These contain both the results for magnetization curve and hysteresis loop. analysis.

REFERENCES

1. Rainville, E.D.
   Special functions, (The MacMillan Co. N.Y., 1960).

2. Cramér, H.
   The elements of probability theory, (John Wiley and Sons, N.Y., 1961).

3. Stewart, K.H.
   Ferromagnetic Domains, (Cambridge University Press, 1954.)

4. Bates, L.F.
   Modern magnetism, (Cambridge University Press 1961).

5. Kittel, C.
   Introduction to solid state physics. (John Wiley and Sons, N.Y., 1950.

6. Bozorth, R.M.
   Ferromagnetism. (D. Van Nostrand Co. Inc., Princeton, New Jersey, N.Y., 1956).

VITA

NAME	Nasir Uddin Ahmed
BORN	Pakistan, Jan. 1934.

<u>EDUCATED</u>

SECONDARY	St. Joseph's High School Khulna, Pakistan
COLLEGE	Daulatpur College Khulna, East Pakistan
UNIVERSITY	Ahsanullah Engineering College Dacca University, Pakistan
	Harwell Reactor School A.E.R.E., England, U.K.

<u>COURSES</u>

Electrical Engineering

Reactor Engineering

<u>DEGREE</u> B.Sc. (Engg.)